Cell

Matrix Crosslinking Forces Tumor Progression by Enhancing Integrin Signaling

Kandice R. Levental,[1,10] Hongmei Yu,[2,10] Laura Kass,[2] Johnathon N. Lakins,[2] Mikala Egeblad,[4,11] Janine T. Erler,[3,12] Sheri F.T. Fong,[5] Katalin Csiszar,[5] Amato Giaccia,[3] Wolfgang Weninger,[6] Mitsuo Yamauchi,[7] David L. Gasser,[8] and Valerie M. Weaver[1,2,4,9,*]

[1]Department of Bioengineering and Institute for Medicine and Engineering, University of Pennsylvania, Philadelphia, PA 19104, USA
[2]Center for Bioengineering and Tissue Regeneration, Department of Surgery, University of California, San Francisco, San Francisco, CA 94143, USA
[3]Department of Radiation Oncology, Stanford University School of Medicine, Stanford, CA 94305, USA
[4]Department of Anatomy, University of California, San Francisco, San Francisco, CA 94143, USA
[5]Cardiovascular Research Center, John A. Burns School of Medicine, University of Hawaii at Manoa, Honolulu, HI 96822, USA
[6]Immunology Program, Wistar Institute, Philadelphia, PA 19104, USA
[7]Dental Research Center, University of North Carolina, Chapel Hill, Chapel Hill, NC 27599, USA
[8]Department of Genetics, University of Pennsylvania, Philadelphia, PA 19104, USA
[9]Department of Bioengineering and Therapeutic Sciences, Eli and Edythe Broad Center of Regeneration Medicine and Stem Cell Research, and Helen Diller Comprehensive Cancer Center, University of California, San Francisco, San Francisco, CA 94143, USA
[10]These authors contributed equally to this work
[11]Present address: Cold Spring Harbor Laboratory, Cold Spring Harbor, NY 11724, USA
[12]Present address: Section of Cell and Molecular Biology, The Institute of Cancer Research, London SW3 6JB, UK
*Correspondence: valerie.weaver@ucsfmedctr.org
DOI 10.1016/j.cell.2009.10.027

SUMMARY

Tumors are characterized by extracellular matrix (ECM) remodeling and stiffening. The importance of ECM remodeling to cancer is appreciated; the relevance of stiffening is less clear. We found that breast tumorigenesis is accompanied by collagen crosslinking, ECM stiffening, and increased focal adhesions. Induction of collagen crosslinking stiffened the ECM, promoted focal adhesions, enhanced PI3 kinase (PI3K) activity, and induced the invasion of an oncogene-initiated epithelium. Inhibition of integrin signaling repressed the invasion of a premalignant epithelium into a stiffened, crosslinked ECM and forced integrin clustering promoted focal adhesions, enhanced PI3K signaling, and induced the invasion of a premalignant epithelium. Consistently, reduction of lysyl oxidase-mediated collagen crosslinking prevented MMTV-Neu-induced fibrosis, decreased focal adhesions and PI3K activity, impeded malignancy, and lowered tumor incidence. These data show how collagen crosslinking can modulate tissue fibrosis and stiffness to force focal adhesions, growth factor signaling and breast malignancy.

INTRODUCTION

The tumor stroma is characterized by extracellular matrix (ECM) remodeling and stiffening, and tissue stiffness has been exploited to detect cancer (Butcher et al., 2009; Sinkus et al., 2000). ECM stiffness enhances cell growth and survival and promotes migration (Lo et al., 2000), and ECM rigidity disrupts tissue morphogenesis by increasing cell tension (Paszek et al., 2005). Reduction of cell tension repressed the malignant behavior of mammary epithelial cells (MECs) and normalized the behavior of breast cancer cells in culture (Paszek et al., 2005). What drives ECM stiffening in tumors and whether ECM tension could drive tumor progression has yet to be determined.

Collagen is the most abundant ECM scaffolding protein in the stroma and contributes significantly to the tensile strength of tissue (Kolacna et al., 2007). Collagen metabolism is deregulated in cancer, where increased collagen expression, elevated deposition, altered organization, and enhanced matrix metalloproteinase (MMP) activity and collagen turnover have been implicated in tumor progression (Jodele et al., 2006). MMP-mediated collagen remodeling can create space for cells to migrate, produce substrate cleavage fragments with independent biological activity, modify adhesion to regulate tissue architecture, and activate, deactivate, or alter the activity of signaling molecules (Page-McCaw et al., 2007). Although high levels of MMPs correlate with poor prognosis in cancer patients (Tetu et al., 2006) and modulation of MMP activity changes tumor phenotype (Zhang et al., 2008), MMP inhibitors failed clinically (Coussens et al., 2002), indicating other ECM remodeling parameters regulate malignancy.

Type I collagen is considered a structural barrier against tumor invasion, but paradoxically, increased expression of collagen is associated with elevated incidence of metastasis (Ramaswamy et al., 2003). Indeed, mammographic density, which is characterized by higher collagen I, increases breast cancer risk (Martin

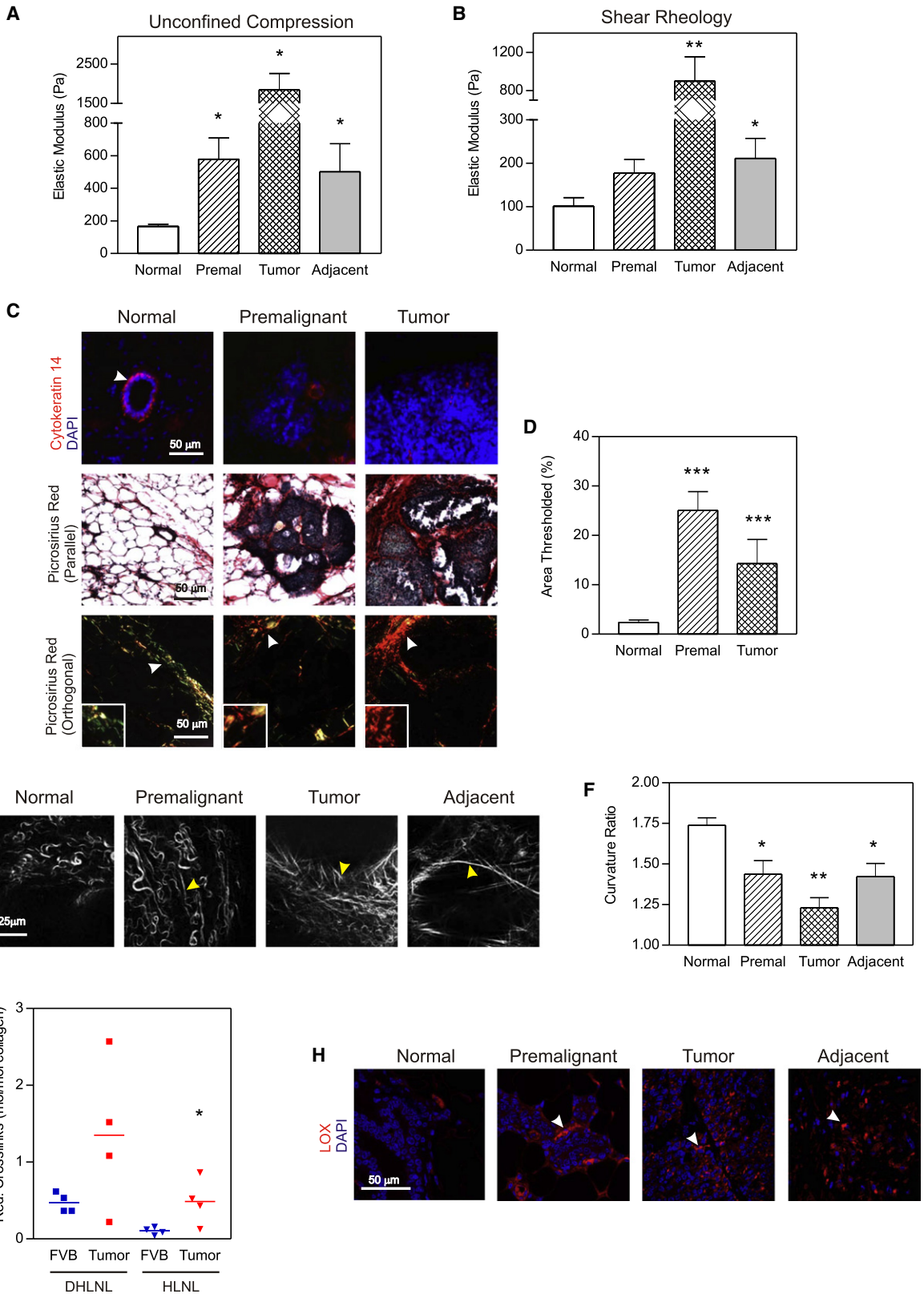
A
Unconfined Compression
Elastic Modulus (Pa)
2500
1500
800
600
400
200
0
Normal
Premal
Tumor
Adjacent
B
Shear Rheology
Elastic Modulus (Pa)
1200
800
300
200
100
0
C
Normal
Premalignant
Tumor
Cytokeratin 14
DAPI
Picrosirius Red
(Parallel)
Picrosirius Red
(Orthogonal)
50 μm
D
Area Thresholded (%)
40
30
20
10
0
E
Normal
Premalignant
Tumor
Adjacent
SHG
25μm
F
Curvature Ratio
2.00
1.75
1.50
1.25
1.00
G
Red. Crosslinks (mol/mol collagen)
3
2
1
0
FVB
Tumor
DHLNL
HLNL
H
Normal
Premalignant
Tumor
Adjacent
LOX
DAPI

and Boyd, 2008). Importantly, collagen crosslinking accompanies tissue fibrosis (van der Slot et al., 2005), and fibrosis increases risk of malignancy (Colpaert et al., 2003). Lysyl oxidase (LOX), a copper-dependent amine oxidase (Kagan and Li, 2003) that initiates the process of covalent intra- and intermolecular crosslinking of collagen by oxidatively deaminating specific lysine and hydroxylysine residues located in the telopeptide domains (Yamauchi and Shiiba, 2008), is frequently elevated in tumors (Erler et al., 2009). Active LOX stiffens tissues and can compromise their function (Pfeiffer et al., 2005), and reduction of LOX activity tempers tissue stiffness and prevents fibrosis (Georges et al., 2007). Nevertheless, the relationship between collagen crosslinking, tissue fibrosis and tension, and cancer has yet to be assessed.

Integrins transduce cues from the ECM by assembling adhesion plaque complexes that initiate biochemical signaling and stimulate cytoskeletal remodeling to regulate cell behavior (Miranti and Brugge, 2002). Force increases integrin expression, activity, and focal adhesions (Paszek et al., 2005; Sawada et al., 2006). Human breast tumors are often fibrotic and stiff, and breast cancer cells that exhibit high tension have elevated integrins and focal adhesions and increased integrin signaling (Madan et al., 2006; Mitra and Schlaepfer, 2006). Thus, ECM stiffness could regulate malignancy by enhancing integrin-dependent mechanotransduction. Consistently, breast malignancy can be inhibited by genetically ablating integrin expression (White et al., 2004), and breast cancer cell behavior can be repressed by inhibition of integrin activity or reduction of cell tension (Paszek et al., 2005). Likewise, knockdown of the expression or inhibition of the function of focal adhesion kinase (FAK) or ^{p130}Cas, two integrin adhesion plaque proteins, impedes breast tumor progression (Cabodi et al., 2006; Lahlou et al., 2007). Here, we asked whether collagen crosslinking could stiffen the ECM and induce fibrosis to promote breast malignancy by altering integrins and whether inhibition of collagen crosslinking could prevent fibrosis and impede breast tumorigenesis by reducing integrin signaling.

RESULTS

ECM Stiffening and Collagen Crosslinking Accompany Breast Tumor Progression

The *HER2* gene is a member of the epidermal growth factor receptor (EGFR) family that is amplified in 20%–25% of human breast cancers. The rat equivalent of *HER2* is the wild-type *Neu* transgene, which, under the MMTV promoter (MMTV-Neu), develops breast tumors with a long latency (Kim and Muller, 1999). Using the MMTV-Neu model, we studied the relationship between tissue fibrosis, stiffness, and cancer. Unconfined compression and rheological testing showed an incremental stiffening of the mammary gland as it transitioned from normal to premalignant to invasive cancer (Figures 1A–1C, top) and demonstrated that the stromal tissue adjacent to the invading epithelium was also substantially stiffer than normal. Total levels (Figure S1 available online) and amount of fibrillar collagen increased markedly (Figures 1C and 1D), and second harmonics generation (SHG) imaging revealed the progressive linearization of the collagen adjacent to the developing epithelial lesions (Figures 1E and 1F).

We next explored whether collagen crosslinking could account for the dramatic ECM remodeling and stiffening. We noted an increase in the levels of the major reducible bifunctional collagen crosslinks, dehydrodihydroxylysinonorleucine (DHLNL), and hydroxylysinonorleucine (HLNL) in the breast tumors, reflecting elevated crosslinked collagen (Figure 1G). We further detected increased amounts of the amine oxidase crosslinking enzyme, LOX, in the stromal cells of the premalignant Min foci and invasive tumors and in the invading transformed epithelium (Figure 1H). These data establish an association between collagen crosslinking, LOX expression, ECM stiffness, and tissue fibrosis in Neu-induced breast tumorigenesis.

LOX-Mediated Collagen Crosslinking and Tissue Stiffening Promote Focal Adhesions and Tumor Progression In Vivo

We next asked whether LOX-mediated collagen crosslinking could stiffen the breast and promote invasion of a premalignant lesion. We used Ha-ras human MCF10AT MECs which upon injection into mice develop into premalignant tissues (Hu et al., 2008). We conditioned inguinal mammary fat pads of NOD/SCID mice, surgically cleared of their epithelium, with control fibroblasts or those expressing elevated LOX (Figures 2A, S2, and S3). Rheological measurement revealed that the mammary glands conditioned with LOX expressing fibroblasts were stiffer (Figure 2B), picrosirius red staining showed that they had more fibrillar collagen (Figures 2C and 2D), and SHG imaging revealed that they had more linearized collagen (Figures 2C and 2E). Consistent with ECM stiffening, resident fibroblasts in the epithelial-cleared LOX-treated glands showed more FAK^{pY397} and ^{p130}Cas immunostaining, indicative of increased focal adhesions and mechanosignaling in the stromal cells (Figure 2C, bottom).

LOX preconditioning and stiffening of the mammary gland promoted the growth and invasion of Ha-ras premalignant

Figure 1. ECM Stiffening, Collagen Crosslinking, and Tissue Fibrosis Accompany Breast Transformation

(A) Elastic modulus of mammary glands from FVB MMTV-Neu mice at different stages of tumor progression measured by unconfined compression.

(B) Shear rheology of tissues described in (A).

(C) Top row: confocal images of tissues in (A) stained for cytokeratin 14 (red) and DAPI (nuclei; blue). Middle and bottom rows: photomicrographs of tissues in (A) stained with picrosirius red and hematoxylin, viewed under parallel (middle) and orthogonal polarizing filters (bottom).

(D) Quantification of images in (C).

(E) SHG images of tissues described in (A).

(F) Quantification of images in (E).

(G) Scatter plot of collagen crosslinks.

(H) Confocal images of tissues described in (A) stained for lysyl oxidase (LOX, red) and DAPI (nuclei, blue). Images are at 40×. Scale bars represent 25–50 μm. Values in (A), (B), and (D) are shown as mean ± standard error of the mean (SEM) of four to six glands/condition. *$p \leq 0.05$, **$p \leq 0.01$, ***$p \leq 0.001$.

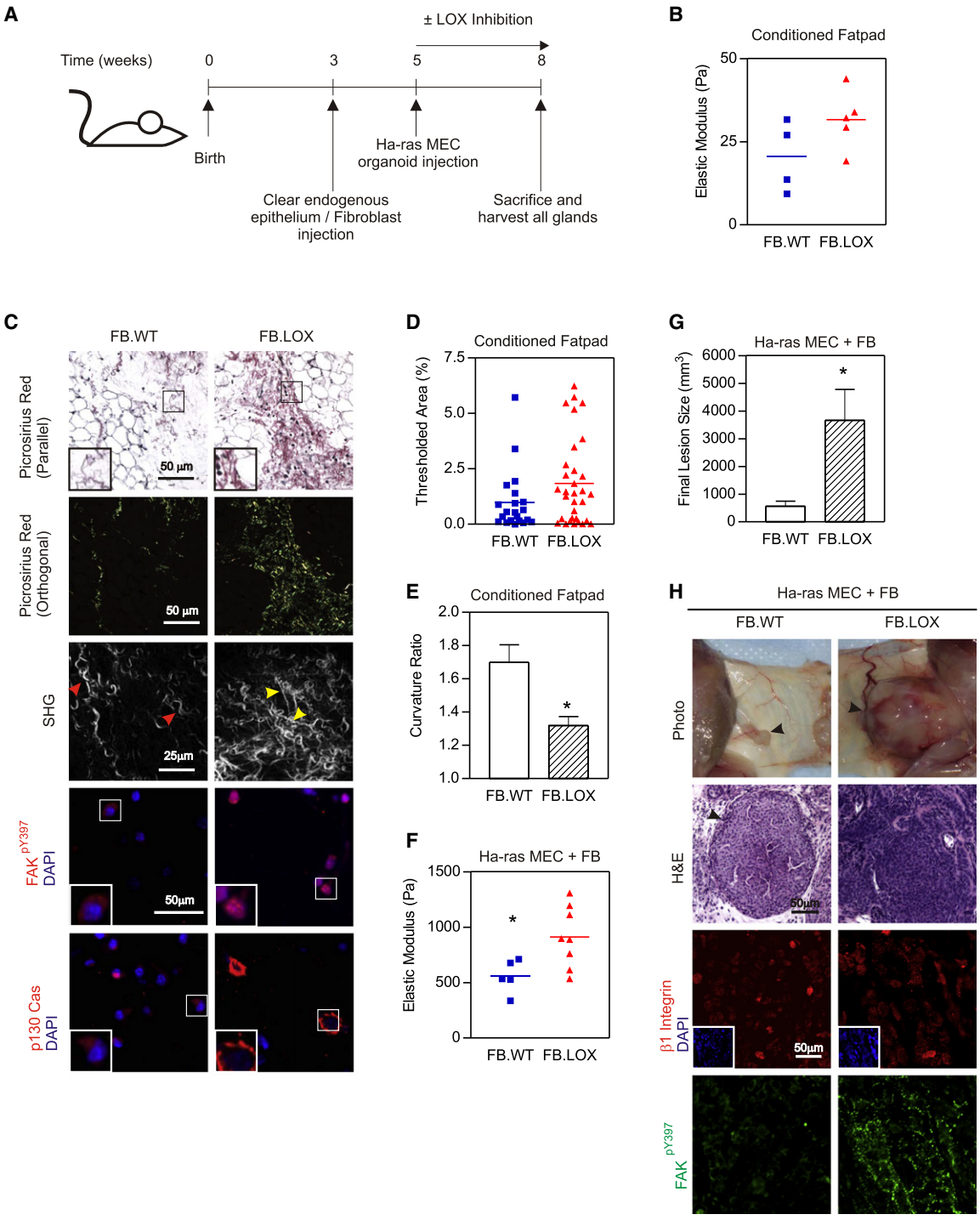

Figure 2. Collagen Remodeling and Tissue Stiffening Promote Focal Adhesions and Tumor Invasion

(A) Experimental design.

(B) Scatter plot of breast rheology after LOX (FB.LOX) or control (FB.ctrl) fibroblast conditioning.

(C) Top two panels: photomicrographs of tissues described in (B) stained with picrosirius red and hematoxylin viewed under parallel and orthogonal polarizing filters. Scale bars represent 50 μm. Third panel: SHG images of tissues from fibroblast-conditioned mammary glands. The scale bar represents 25 μm. Fourth and fifth panels: confocal images of fibroblasts residing within fibroblast-conditioned mammary glands stained for active FAK (FAK^{pY397}, red, fourth panel), ^{p130}Cas (red, fifth panel), and DAPI (nuclei, blue). The scale bar represents 50 μm.

(D) Scatter plot of fibrillar collagen in tissue shown in (C).

(E) Scatter plot of collagen linearity measured by curvature ratio from SHG images shown in (C).

mammary organoids injected into these tissues as revealed by a significant increase in lesion size and tumors that lacked margins (Figures 2F–2H). MECs in the LOX preconditioned glands also had more focal adhesions, as revealed by elevated FAK^{pY397} (Figure 2H) and ^{p130}Cas (data not shown). To rule out any direct effect of LOX activity on MEC behavior, we also treated a cohort of animals in parallel (i.e., at time of MEC injection) with β-aminopropionitrile (BAPN), a natural and irreversible inhibitor of lysyl oxidase activity (Kagan and Li, 2003). Because BAPN treatment had no effect on tumor growth, invasion, and focal adhesions (Figures S4–S6), we concluded that it was LOX preconditioning of the stroma and ECM stiffness that promoted mammary tumor progression, and not any direct effect of LOX on the mammary epithelium. These findings demonstrate how ECM crosslinking and stiffening can induce focal adhesions and promote the growth and invasion of an oncogene-initiated mammary epithelium in vivo.

Inhibition of LOX-Mediated Collagen Crosslinking Decreases Fibrosis and Reduces Focal Adhesions to Inhibit Breast Tumor Progression In Vivo

We next asked whether reduction of LOX-dependent collagen crosslinking could temper tissue fibrosis and decrease focal adhesions, and whether this would inhibit breast tumor progression. We inhibited LOX activity using the cell-soluble BAPN (Lucero and Kagan, 2006) or a LOX-specific function-blocking polyclonal antibody that only inhibits extracellular LOX activity (Erler et al., 2006) and assayed collagen crosslinking, tissue fibrosis, focal adhesions, and breast tumor development.

Inhibition of LOX activity was initiated in five month old parous animals, when LOX levels were already increased in the stromal cells but were non-detectable in the mammary epithelium (Figure 1H). Treatment was continued for 1 month, after which the animals were allowed to recover for another month and then sacrificed (Figure 3A). At the time of sacrifice, the non-treated MMTV-Neu mice had high levels of active LOX in the serum, whereas BAPN or LOX-inhibitory polyclonal antibody-treated animals had reduced levels (Figure 3B). Mice with reduced LOX activity showed significant decreases in LOX-mediated collagen crosslinks, both reducible (DHLNL and HLNL) and nonreducible (pyridinoline) (Figures 3C and 3D), and the collagen fibrils adjacent to the epithelial lesions were less linear (Figures 3E and 3F). Consistent with the possibility that inhibition of collagen crosslinking prevented tissue fibrosis, LOX inhibition reduced fibrillar collagen (Figures 3G and 3H) and had less focal adhesions, as indicated by negligible FAK^{pY397} (Figure 3I).

Inhibition of LOX activity also increased tumor latency (Figure 4A) and decreased tumor incidence (Figure 4B), despite ErbB2 activity (Figure 4C). Moreover, the palpable lesions formed in the LOX-inhibited animals were smaller (Figure 4D) and less proliferative (Figure 4E). LOX-inhibited mammary glands also stained positively for cytokeratin 14 along the basal periphery of the ducts, implying retention of their myoepithelium (Figures 4H and 4I). Hematoxylin and eosin (H&E) sections revealed that a significantly greater proportion of the lesions in the LOX-inhibited animals were hyperplastic or premalignant (hyperplastic alveolar nodules [HANs] or mammary intraepithelial neoplasias [MINs]) and the tumors that did develop were mostly low grade as opposed to the high grade carcinomas typically observed in the untreated Neu mice (Figures 4G and 4F). These results show how inhibition of LOX activity reduces collagen crosslinking, tempers tissue fibrosis, decreases focal adhesions, and impedes tumor progression to reduce breast tumor incidence.

Collagen Crosslinking and ECM Stiffening Promote Focal Adhesions and Drive Invasion of Oncogenically Initiated Mammary Tissues in Culture

We next assessed the effect of nonspecific induction of collagen crosslinking and stiffening on MEC invasion in the absence of fibroblasts, immune cells, and other stromal and systemic cellular and soluble factors (Figure 5A, experimental design). We explored the effect of nonspecific collagen crosslinking and stiffening on tumor invasion by adding ribose to the media of nonmalignant, MCF10A acini embedded in a 3D soft collagen I/reconstituted basement membrane gel (Col/rBM gel).

To determine whether MEC invasion required oncogenic signaling, we utilized MCF10As expressing an ErbB2 chimera (ErbB2.chim; called HER-2; the human homolog of Neu) consisting of the extracellular and transmembrane domains of low-affinity nerve growth factor receptor (p75NGFR), and the cytoplasmic kinase domain of ErbB2 linked to the synthetic ligand-binding domain from the FK506-binding protein (FKBP). In these MECs, addition of the synthetic bivalent FKBP ligand, AP1510, drives homodimerization of ErbB2, activation of the kinase domain, and initiation of ErbB2 signaling (Muthuswamy et al., 2001). Chimeric ErbB2 signaling drives proliferation and luminal filling but fails to induce MEC invasion in rBM (Figure 5E). To study effects of homo- (ErbB2/ErbB2) and heterodimer (ErbB1/ErbB2) formation, we also engineered MECs in which the wild-type ErbB2 could be overexpressed through addition of doxycycline (ErbB2.TetOn; Figures S7 and S8).

In the absence of ErbB2 activity, MECs in collagen/rBM gels assembled acini, as illustrated by basally oriented β4 integrin and cell-cell localized beta catenin (Figure 5E). Glycation-mediated crosslinking stiffened the collagen (Figure 5B), increased colony size (Figure 5C), and disrupted tissue organization, as revealed by diffusely localized beta catenin and the appearance of random cells within the lumens (Figure 5E). MECs within the ribose crosslinked collagen gels also had elevated levels and co-localized β1 integrin and FAK^{pY397}, indicative of tension-induced

(F) Rheology of mammary glands with injected Ha-ras MCF10AT MECs.
(G) Lesion burden for mouse cohorts.
(H) Top: photographs of mammary glands 3 weeks after injection with Ha-ras MCF10AT organoids. Middle: H&E-stained tissue of MECs from lesions shown in (H). Bottom: confocal images of MECs in tissue shown in (H) stained for β1 integrin (red), active FAK (FAK^{pY397}, green) and DAPI (nuclei, blue, inset). Scale bars represent 50 μm.
Values in (E) and (G) are mean ± SEM of several glands. *$p \leq 0.05$.

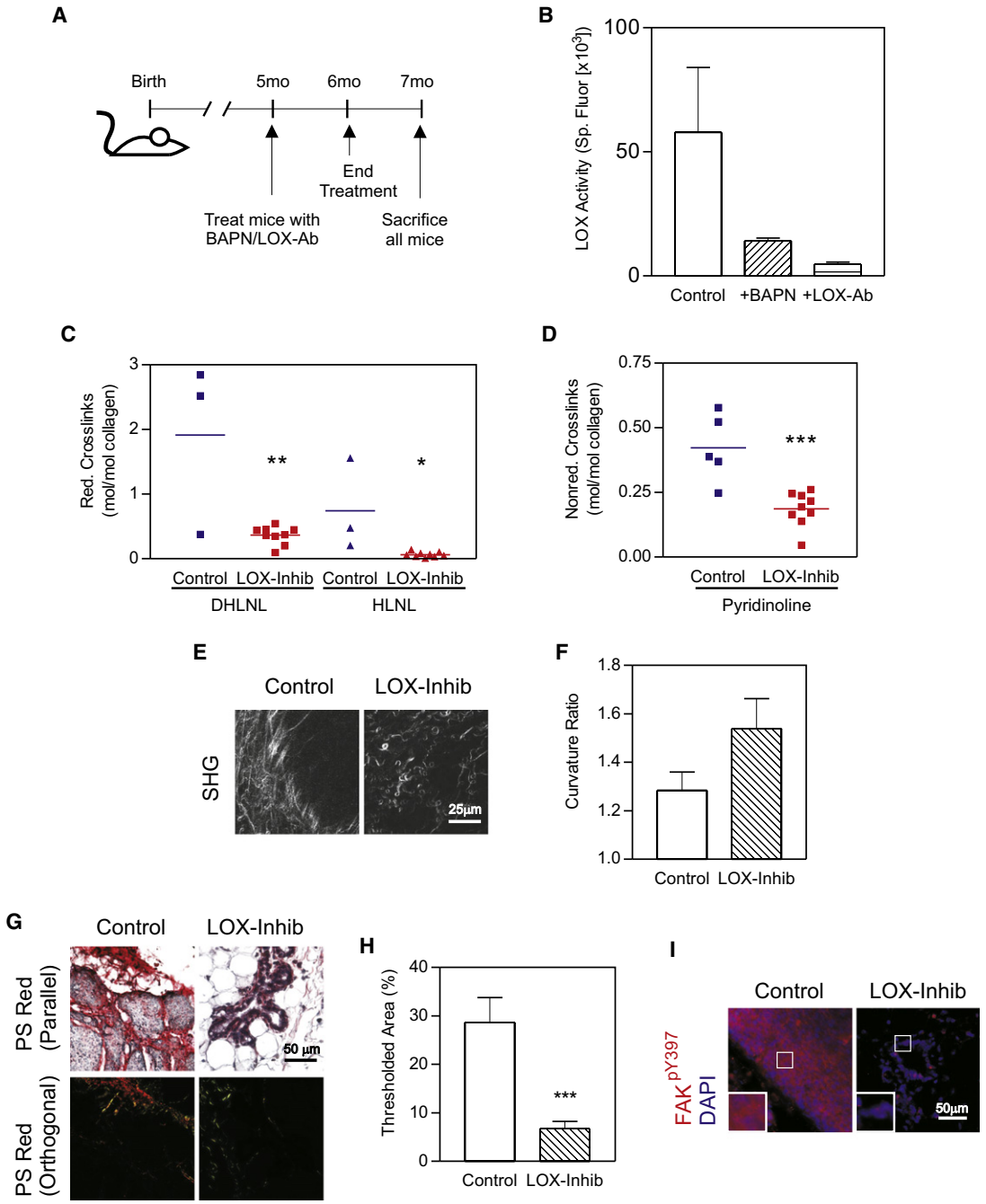

Figure 3. Inhibition of Collagen Crosslinking Tempers Tissue Fibrosis and Reduces Focal Adhesions

(A) Experimental design.

(B) LOX enzymatic activity in serum of untreated (Control) compared to BAPN (+BAPN) or LOX-inhibitory antibody-treated (+LOX-Ab) Neu mice. Values are shown as mean ± SEM.

(C) Scatter plots of reducible collagen crosslinks in LOX-inhibited (LOX-Inhib) and untreated (Control) Neu breasts.

(D) Scatter plots of pyridinoline in LOX-inhibited (LOX-Inhib) and untreated (Control) Neu breasts.

(E) SHG images of mammary glands from BAPN-treated animals as described above. The scale bar represents 25 μm.

(F) Collagen curvature in SHG images from (D) (Supplemental Experimental Procedures). Data are mean ± SEM of three to five regions/four glands/condition.

(G) Photomicrographs of sections from control and BAPN-treated (LOX-Inhib) Neu mammary glands stained with picrosirius red and hematoxylin viewed under parallel or orthogonal polarizing filters. The scale bar represents 50 μm.

(H) Fibrillar collagen in control and LOX-inhibited glands from images shown in (F). Data are mean ± SEM of four to six images/four to eight glands/condition.

(I) Confocal images of sections from control and BAPN-treated Neu glands stained for active FAK (FAK^{pY397}, red) and DAPI (nuclei, blue). The scale bar represents 50 μm.

*$p \leq 0.05$, **$p \leq 0.01$, ***$p \leq 0.001$.

focal adhesions (Figure 5D). Nevertheless, in the absence of ErbB2 activity, ECM stiffening did not drive MEC invasion (Figures 5E and 5F).

Addition of either AP1510 (1 μM) or doxycycline (0.2 μg/mL) to the mammary acini, induced and activated (ErbB2.TetOn) or directly activated ErbB2 (ErbB2.chim) (Figure S9), promoted cell growth (data not shown), drove luminal filling, and destabilized cell-cell junctions, as revealed by diffusely localized beta catenin (Figure 5E). Sustained ErbB2 activation did not drive MEC invasion, as indicated by colony integrity and the retention of basally localized β4 integrin (Muthuswamy et al., 2001) (Figures 5E and 5F). Yet, when ErbB2 was activated in colonies in the crosslinked, stiffened gels, colony architecture disintegrated, as revealed by the absence of detectable beta catenin and disorganized β4 integrin staining, and MECs invaded into the gels (Figure 5E, white arrows; quantified in Figure 5F). SHG imaging revealed that individually, ErbB2 activation and ECM stiffening were accompanied by the appearance of prominent collagen bundles surrounding the colonies and showed that MECs with activated ErbB2 invaded on fibrils that extended perpendicularly into the crosslinked, stiffened gels (Figurs 5E, white arrows highlight an invasive MEC, yellow arrows indicate collagen reorganization; Figure S9). These findings show how collagen crosslinking and ECM stiffening, per se, cooperate with oncogenes such as ErbB2 to promote the invasive behavior of a mammary epithelium.

Interestingly, confocal imaging revealed elevated ^{p130}Cas and FAK^{pY397} staining that colocalized with β1 integrin (colocalization analysis of FAK^{pY397} and β1 integrin; Pearson's r = 0.78; ^{p130}Cas and β1 integrin, Pearson's r = 0.89) in the stiffer breast tissue of the Neu mice (Figure 6A; see insert) and reduced levels of FAK^{pY397} after LOX inhibition (Figure 3H). Moreover, inhibition of β1 integrin activity, with the function blocking antibody AIIB2, or reduction of integrin signaling by expression of an inducible FRNK (FRNK.TetOn; Figure S10) prevented the force-mediated invasion of the ErbB2 activated mammary organoids (Figures 5G and 5H). These findings show how ECM crosslinking and stiffness cooperate with an oncogene to promote breast cell invasion and implicate integrin signaling in force-dependent tumor progression.

Integrin Clustering Promotes Focal Adhesions to Drive Invasion of a Ha-ras Mammary Epithelium In Vitro and In Vivo

To determine whether integrin signaling would be sufficient to induce breast tumor invasion, we expressed a series of integrin constructs in nonmalignant MCF10A and Ha-ras premalignant MCF10AT MECs and assayed for invasive behavior in rBM and in vivo (Figure 6B).

Expression of the V737N integrin, which recapitulates tension-dependent integrin clustering, promoted focal adhesions, indicated by elevated FAK^{pY397} (Figure 6C), and disrupted the integrity of mammary colonies in rBM, revealed by luminal filling and altered β4 integrin localization (Figure 6C, top). In contrast, expression of neither a wild-type (Figure 6C) nor a constitutively active β1 integrin (not shown; Paszek et al. [2005]) induced focal adhesions and disrupted mammary tissue architecture. Moreover, while the V737N β1 integrin mutant failed to promote invasion of the MCF10A MECs (Figure 6C), the V737N integrin induced the invasion of the Ha-ras premalignant MCF10AT colonies in rBM (Figures 6D and 6E). Upon injection into nude mice, the V737N integrin not only promoted focal adhesions and increased lesion size (Figure 6F), but also induced the invasive behavior of the Ha-ras MCF10AT organoids, as revealed by the loss of epithelial lesion margins and increased FAK^{pY397} (see arrows in Figure 6G). These findings implicate tension-dependent integrin clustering and focal adhesions in breast tumor invasion. However, because integrin clustering could only promote invasion in Ha-ras premalignant MECs, they also illustrate how integrin-mediated mechanotransduction cooperates with oncogenic signaling to drive malignancy.

Collagen Crosslinking and Tissue Stiffness Promote Integrin Clustering and Enhance PI3K Signaling to Regulate Invasion of a Premalignant Mammary Epithelium In Vitro and Tumor Progression In Vivo

Integrins activate PI3K, and PI3K promotes invasion in culture and tumor progression in vivo (Webster et al., 1998). Therefore, we explored the relationship between focal adhesions and PI3K signaling in tension-dependent breast tumor invasion. We found Akt signaling, an established target of PI3K, to be elevated in the premalignant and malignant, rigid mammary tissue (Figure 7A) and in the mammary colonies in the ribose-stiffened collagen gels (Figure 7B).

We examined the effect of ECM rigidity on PI3K activity in MECs plated on rBM-functionalized polyacrylamide gels (rBM PA gel) with elastic moduli of 140–400 (soft) and ≥5000–10,000 (stiff) Pascals. These two extremes represent the ECM stiffness of healthy versus transformed breast tissue. Although substrate stiffness did not increase the levels of Akt^{pS473} in unstimulated MECs, ECM stiffness potentiated the magnitude of EGF-activated Akt^{pS473} (Figure 7C) and increased ErbB2-activated Akt^{pS473} (Figure 7D). MECs on soft gels that expressed the β1 integrin cluster mutant, but not the wild-type β1 integrin, also showed a significant increase in Akt^{pS473} activity after EGF stimulation. These results suggest that integrin mechanotransduction potentiates growth factor dependent PI3 kinase signaling (Figures 6B, 6C, and 7E).

Pharmacological inhibition of PI3K activity with LY294002 restored the colony architecture of ErbB2-activated MECs in ribose crosslinked collagen gels toward that of a noninvasive, polarized, cohesive colony (Figures 7F and 7G). Inhibition of PI3K activity reduced colony size, and immunostaining revealed that colonies treated with LY294002 retained β catenin at cell-cell junctions and had basally localized β4 integrin (Figure 7F). The epithelium from the LOX-inhibited Neu mice also had lower PI3K signaling, as revealed by fainter active Akt/PI3K substrate staining (Figure 7H). These data are consistent with a role for integrin mechanotransduction in PI3K-mediated breast tumor invasion. The findings suggest that ECM stiffness, as induced by elevated collagen crosslinking could promote breast malignancy by enhancing integrin-GFR crosstalk (Figure 7I) (Miranti and Brugge, 2002).

DISCUSSION

Our findings identify collagen crosslinking as a critical regulator of desmoplasia and imply that the level and nature of ECM

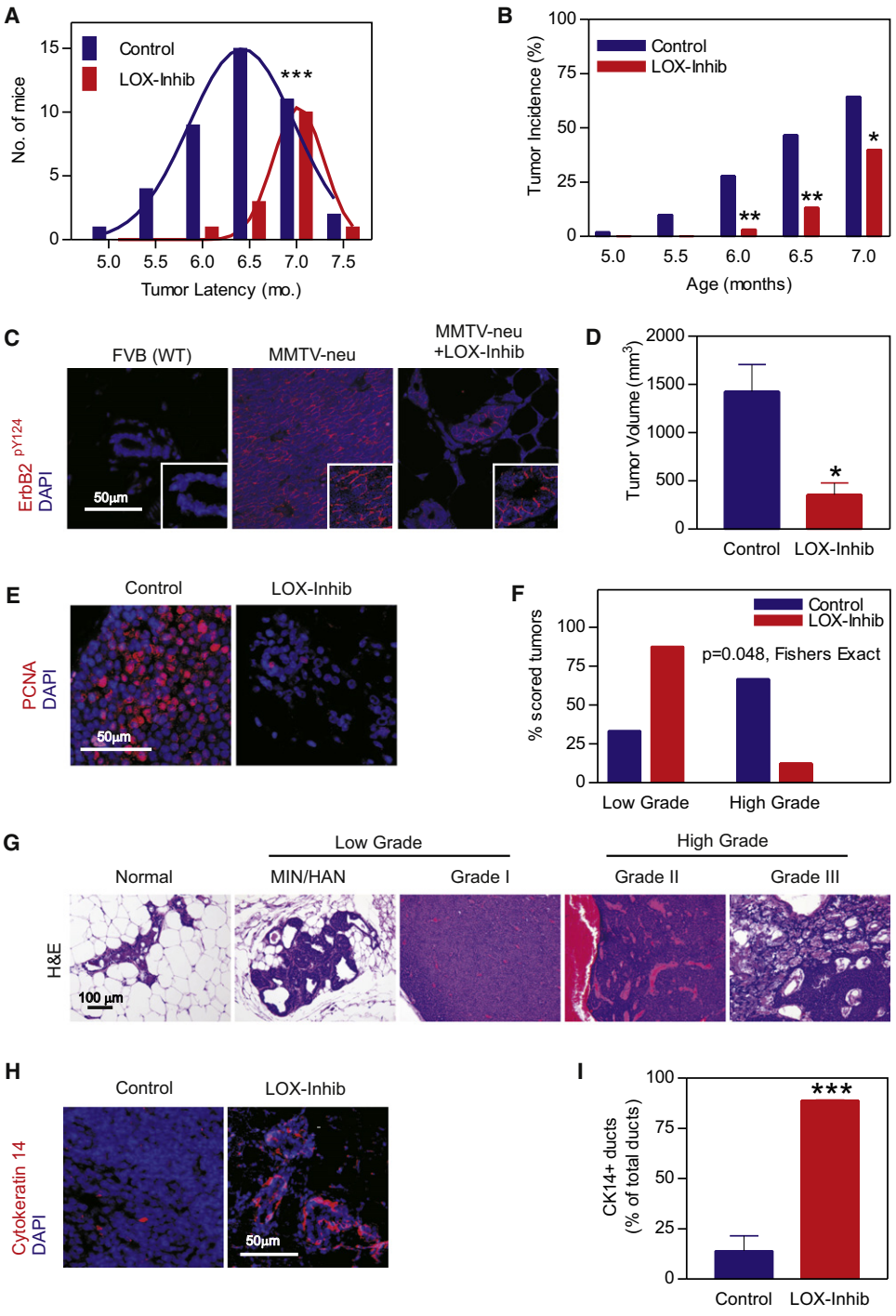

Figure 4. Inhibition of Crosslinking Reduces Tissue Fibrosis and Tumor Incidence and Enhances Tumor Latency

(A) Tumor latency.

(B) Tumor incidence without (Control) or with (LOX-Inhib) LOX inhibition.

(C) Confocal images of activate ErbB2 (ErbB2^{pY1248}, red) in tissues from FVB nontransgenic littermates, Neu (MMTV-Neu) and LOX-inhibited mice (MMTV-Neu +LOX-Inhib). The scale bar represents 50 μm.

(D) Tumor size in control and LOX-inhibited mice.

(E) Confocal images of sections from LOX-inhibited and control glands stained for PCNA (red) and DAPI (nuclei, blue). The scale bar represents 50 μm.

(F) Grading of tumor lesions from mammary glands of control (n = 14) and BAPN-treated (LOX-Inhib, n = 13) animals.

(G) H&E-stained tissue showing typical normal glandular structure, hyperplastic alveolar nodules (HANs), and mammary intraepithelial neoplasias (MINs) premalignant lesions and grades I, II, and III ductal tumors.

crosslinks in a tissue could impact cancer risk and alter tumor behavior. The observations are consistent with links between ECM crosslinking and tissue stiffening in tissue fibrosis and could explain the increased risk to malignancy associated with these conditions (Colpaert et al., 2003). They might also explain why women with mammographically dense breasts have an increased relative risk of developing cancer (Martin and Boyd, 2008). Because aged tissues are stiffer and contain high levels of aberrant collagen crosslinks, the data offer a new paradigm for understanding why tumor incidence increases so dramatically with aging (Szauter et al., 2005).

Tissue fibrosis influences tumor progression by regulating soluble factors that induce inflammation and angiogenesis and stimulate cell growth and invasion (Bierie et al., 2009; Coussens et al., 1999). We showed that modification of the state of collagen crosslinking and ECM stiffness, two physical parameters of the tissue microenvironment, modulated the invasive behavior of an oncogene pre transformed mammary epithelium, even in the absence of cellular and soluble tissue and systemic factors. The findings imply that tissue fibrosis could regulate cancer behavior by influencing the biophysical properties of the microenvironment to alter force at the cell and/or tissue level. Importantly, we noted that focal adhesions were elevated in the stiffened breast tumors and organoid cultures, that forcing focal adhesions promoted MEC invasion, and that inhibiting focal adhesion signaling or tempering tissue stiffening reduced focal adhesions and tumor invasion. These observations are consistent with the notion that force regulates the invasive behavior of tumors by modulating integrin activity and focal adhesion assembly and signaling (Paszek et al., 2005). The findings thereby provide an explanation for why ^{pY}FAK and ^{p130}Cas are so often increased in breast tumors (Cabodi et al., 2006; Madan et al., 2006), even when integrin expression is frequently decreased (Koukoulis et al., 1993; Zutter et al., 1998). Indeed, the observations suggest that enhanced integrin signaling rather than just an increase in integrin expression is more critical for tumor progression.

Our data show how modulating the activity of one class of ECM crosslinking enzymes, the LOXs, can directly modify tumor progression by regulating collagen crosslinking and stiffness. The results are consistent with data indicating that LOX enzymes are elevated in many cancers (Erler and Weaver, 2009) and that LOX is induced by hypoxia inducible factor (HIF-1) and TGFβ, two key regulators of tumor behavior (Postovit et al., 2008). Indeed, cellular LOX promotes breast cell migration and invasion and enhances tumor proliferation and survival (Kirschmann et al., 2002). Hypoxia-induced LOX modulates tumor metastasis by regulating integrin function (Erler and Giaccia, 2006) by facilitating tumor extravasation (Bondareva et al., 2009) or by conditioning the metastatic niche (Erler et al., 2009). Our work indicates that LOX can promote tumor progression and MEC invasion by increasing fibrillar collagen and ECM stiffness. These observations are consistent with the major function of LOX in tissues as a key enzyme for collagen and elastin crosslinking that enhances tensile strength (Szauter et al., 2005). Consistently, by inhibiting LOX activity early, when levels were high in the stroma, we prevented ECM remodeling and stiffening and reduced tumor progression in the MMTV-Neu mice. Because a LOX-specific inhibitory polyclonal that cannot inhibit intracellular LOX also prevented fibrosis and tumor progression, our results suggest that LOX-mediated collagen crosslinking likely regulates breast tumor progression by modifying the tumor microenvironment rather than by directly changing cell behavior.

We observed that LOX inhibition reduced focal adhesions and PI3K signaling indicating that LOX modulates breast tumor progression by stiffening the ECM to drive focal adhesions assembly and enhance GFR-dependent PI3K signaling. Consistently, we showed that ribose-mediated collagen crosslinking, which induces nonspecific collagen glycation, also stiffened the ECM and enhanced focal adhesions and PI3K signaling to promote ErbB2-dependent breast tumor invasion. We noted that MEC invasion could be abrogated by inhibition of integrin and FAK activity, thereby illustrating the importance of ECM crosslinking and stiffness in tumor progression. This idea is consistent with our recent findings that LOX conditioning of the lung ECM promotes breast tumor metastasis (Erler et al., 2009) and data showing that fibrotic breast tumors have the poorest prognosis and highest rate of recurrence (Hasebe et al., 1997). Indeed, our findings underscore the notion that ECM crosslinking and stiffness, per se, is a key regulator of tumor progression. They imply that other ECM crosslinkers/modulators implicated in tissue fibrosis such as tissue transglutaminase, lysyl hydroxylase or some of the proteoglycans or even non-specific metabolic glycation end products (AGEs) might also similarly promote malignancy.

LOX has been proposed to be a tumor suppressor (Payne et al., 2007) possibly by directly inhibiting ECM adhesions and integrin signaling (Zhao et al., 2008). LOX-mediated ECM stiffening could also impede cell invasion in the absence of MMP activity (Zaman et al., 2006) reminiscent of highly crosslinked, stiff fibrotic tissues and scars that often never progress to malignancy. We noted that neither ECM stiffness nor forced integrin clustering induced mammary tissue invasion in the absence of oncogenic signaling. This suggests that other factors that modulate integrins and/or ECM remodeling or cellular tension likely cooperate with ECM crosslinking and force to promote tumor invasion (Katz et al., 2007; Wolf et al., 2007). Instead, ECM stiffness appears to operate as a signaling rheostat potentiating oncogenic cues to promote tumor invasion.

Cancer progression is accompanied by MMP-dependent ECM remodeling. Multiple MMPs are overexpressed in the tumor stroma, and some MMPs are upregulated in transformed epithelia (Jodele et al., 2006; Page-McCaw et al., 2007). Elevated expression of specific MMPs induced desmoplasia and malignant transformation (Sternlicht et al., 1999) and genetic ablation of MMPs or pharmaceutical inhibition of MMP activity reduced breast metastasis (Martin et al., 2008). These data argue that MMPs are critical for malignancy. Nevertheless, clinical trials with MMPs failed, suggesting that the role of MMPs in cancer

(H) Confocal images of breast tissue stained for cytokeratin 14 (red) and DAPI (nuclei, blue) in control and LOX-inhibited tissue. The scale bar represents 50 μm.
(I) Quantification of cytokeratin 14 positive glands in (H) detected in breast from control and LOX-inhibited animals.
Values in (A), (B), (D), (F), and (I) are shown as mean ± SEM of four to six measurements/four to 12 tissue sections/group. *$p \leq 0.05$, **$p \leq 0.01$, ***$p \leq 0.001$.

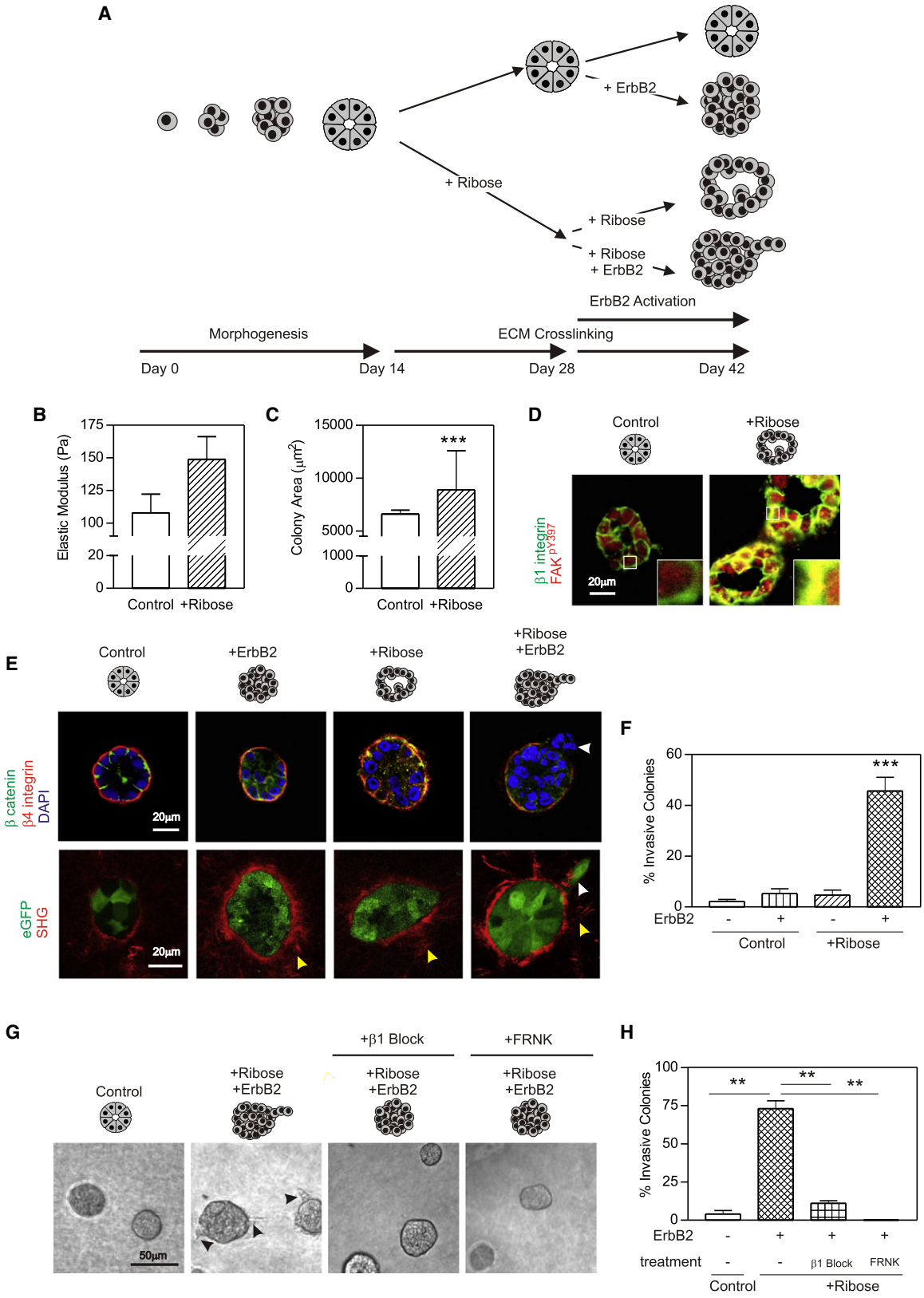
A
+ ErbB2
+ Ribose
+ Ribose
+ Ribose
+ ErbB2
ErbB2 Activation
Morphogenesis
ECM Crosslinking
Day 0
Day 14
Day 28
Day 42
B
Elastic Modulus (Pa)
175
150
125
100
20
0
Control
+Ribose
C
Colony Area (μm²)
15000
10000
5000
1000
0
***
Control
+Ribose
D
Control
+Ribose
β1 integrin
FAK pY397
20μm
E
Control
+ErbB2
+Ribose
+Ribose
+ErbB2
β catenin
β4 integrin
DAPI
20μm
eGFP
SHG
20μm
F
% Invasive Colonies
60
40
20
0
***
ErbB2
-
+
-
+
Control
+Ribose
G
+β1 Block
+FRNK
Control
+Ribose
+ErbB2
+Ribose
+ErbB2
+Ribose
+ErbB2
50μm
H
% Invasive Colonies
100
75
50
25
0
**
**
**
ErbB2
-
+
+
+
treatment
-
-
β1 Block
FRNK
Control
+Ribose

is more complicated (Coussens et al., 2002). Indeed, MMPs collaborate with crosslinking enzymes such as LOX to facilitate collagen maturation, and MMPs and LOX regulate the expression and activity of soluble factors such as transforming growth factor beta (TGFβ) that regulate tumor cell behavior (Atsawasuwan et al., 2008; Csiszar, 2001; Decitre et al., 1998; Szauter et al., 2005). TGFβ in turn regulates the expression of many ECM proteins and modifying enzymes including LOXs, and TGFβ increases levels of factors that evoke inflammation, induce fibrosis and promote metastasis (Bierie and Moses, 2006; Oleggini et al., 2007). Indeed, force itself modulates TGFβ activation and compression alters growth factor signaling (Tschumperlin et al., 2004; Wipff et al., 2007). These findings underscore the dynamic and reciprocal relationship between ECM deposition, processing, degradation, and force. They suggest that cancer is best viewed as a dynamic, phenotypically plastic, and highly coordinated tissue remodeling process that is tightly regulated by biochemical and mechanical cues. Accordingly, not only will we need to clarify the role of ECM cleavage in tumors but we will also be obliged to understand how ECM remodeling is integrated within the context of its deposition, posttranslational modifications, and topological rearrangement and to take into consideration the effect of mechanical force as a key regulator of malignancy.

EXPERIMENTAL PROCEDURES

Antibodies and Reagents

Antibodies were as follows: β4 integrin (3E1); β1 integrin (AIIB2, Chemicon); FAK (77), YES (1), β1 integrin (18), E-Cadherin (610405, BD Transduction); laminin-5 (BM165, MP Marinkovich); β actin (AC-15, Sigma); ErbB2 (3B5, Calbiochem); polyclonal β catenin (Sigma); FAK^{pY397} (BioSource); Phospho-(Ser/Thr) Akt Substrates and Akt^{pS473} (Cell Signaling); Akt (BD PharMingen); p130Cas, ErbB2^{pY1248} (Abcam); cytokeratin 14 (Covance); LOX (A. Giaccia, Stanford University); LOX polyclonal activity inhibitory antibody (OpenBiosystems); and secondary AlexaFluor goat anti-mouse, anti-rabbit, and anti-rat (488 and 555 conjugates), AlexaFluor phalloidin (488 conjugate, Invitrogen); donkey anti-mouse and anti-rabbit (Cy2 and Cy3 conjugates, Jackson ImmunoResearch); and sheep anti-mouse and anti-rabbit HRP-linked (Amersham). Reagents included LY294002 (50 μm in DMSO, Calbiochem).

Cell Manipulations

MEC and fibroblast cell lines were cultured as described (Paszek et al., 2005). Collagen crosslinking was induced by addition of 15 mM ribose to the culture medium (Girton et al., 1999). rBM-conjugated PA gels with calibrated stiffness were prepared as described (Johnson et al., 2007).

Vector Constructs and Gene Expression

Full-length human *ErbB2* (K. Ignatoski) was cloned into the pRet puro Tet IRES EGFP tetracycline-inducible vector. The β1 integrin wild-type, β1 integrin glycan wedge constitutively active, and β1 integrin clustering mutant V737N constructs and the preparation of virus and cell infection and selection have been described (Paszek et al., 2005). Four *myc* tags were added to the C terminus of full-length *LOX* and cloned into the pLV puro TetO$_7$mCMV tetracycline-inducible lentiviral vector and expressed biscistronically with *eGFP*.

Elastic Modulus Measurements

Mammary glands and gels were assayed for materials properties by unconfined compression and rheometrical analysis (Paszek et al., 2005) (Supplemental Experimental Procedures).

Mice and Treatments

FVB-TgN MMTV-Neu, NOD/SCID, and BalbC nu/nu mice (Jackson Laboratory) were maintained in accordance with University of Pennsylvania and University of California Institutional Animal Care and Use Committee guidelines. For LOX-inhibition studies, animals were treated with BAPN (3 mg/kg; Spectrum) in the drinking water (four to eight mice/group, four studies) or a LOX function-blocking polyclonal antibody (3 mg/kg; OpenBiosystems, D8746) injected intraperitoneally twice per week (three to four mice/group, one study). Mice were sacrificed at 7–7.5 months of age, at which time tail vein blood was collected. Lesions were detected by palpation (~3 mm diameter), and tumor volume was assessed with calipers. At sacrifice mammary glands were excised, imaged, and mechanically tested or snap frozen or paraformaldehyde fixed.

Tumor Grading

Tumor grading was performed blinded on H&E-stained sections from untreated (n = 14) or BAPN-treated (n = 13) #2–3 mammary glands. Premalignant lesions were defined as HAN- or MIN-like foci. Grade I lesions were well defined as homogenous carcinomas, grade II contained areas with strong necrosis, stromal reaction and/or red blood cells outside of tumor blood vessels, and grade III also contained necrosis and nuclear pleiomorphy. Adjacent tissue was defined as mammary tissue surrounding a tumor that was cut away from the tumor prior to subsequent analysis. A small set of anti-LOX-treated mice (n = 4) was compared with their controls (n = 3), and showed they the same tendency to less progressed lesions as was observed in the BAPN-treated animals.

Xenograft Manipulations

NOD/SCID mice (n = 24) were used for mammary fat pad transplantation studies (Kuperwasser et al., 2004). In brief, the rudimentary inguinal epithelium was removed from 3-week-old anesthetized female mice and 5 × 10^5 NIH 3T3 WT or LOX-expressing fibroblasts (2.5 × 10^5 were treated with 4Gy irradiation 24 hr prior to injection) were injected into the left and right mammary glands. Two weeks after fibroblast injection, 1 × 10^6 DCIS.com MCF10AT MEC 4-day-old rBM-generated, proliferating organoids (16–20 cells/organoid) were suspended in Dulbecco's modified PBS and injected into the preconditioned

Figure 5. Collagen Crosslinking and ECM Stiffening Promote Focal Adhesions and Invasion of ErbB2 Mammary Colonies

(A) Experimental design.

(B) Elastic modulus of ribose crosslinked (+Ribose) and untreated (Control) collagen gels.

(C) Cross-sectional area of MEC colonies in +ribose and control gels.

(D) Confocal images of MCF10A colonies stained for β1 integrin (green), activate FAK (FAK^{pY397}, red), and DAPI (nuclei, blue) in control and +ribose gels. The scale bar represents 20 μm.

(E) Top panels: confocal images of MEC colonies expressing the ErbB2 chimera stained for β catenin (green), β4 integrin (red), and DAPI (nuclei, blue) in control or +ribose gels with (+ErbB2) or without ErbB2 activity. Bottom panels: SHG images of collagen fibrils and confocal images of eGFP expressing MEC colonies as described above. Scale bars represent 20 μm. Yellow arrows identify collagen bundles surrounding the colony periphery, and white arrows indicate an invading MEC.

(F) Percent colony invasion shown in (E).

(G) Phase-contrast images of MEC colonies expressing the ErbB2 chimera in control or +ribose gels, with active ErbB2 (+ErbB2), coexpressing a doxycycline-inducible FRNK (right panel) or treated with β1 integrin function-blocking antibody (+β1 block).

(H) Percent colony invasion shown in (G).

Values in (B), (C), (F), and (H) are shown as mean ± SEM from three to five experiments and/or 50–100 colonies in three experiments. $^{**}p \leq 0.01$, $^{***}p \leq 0.001$.

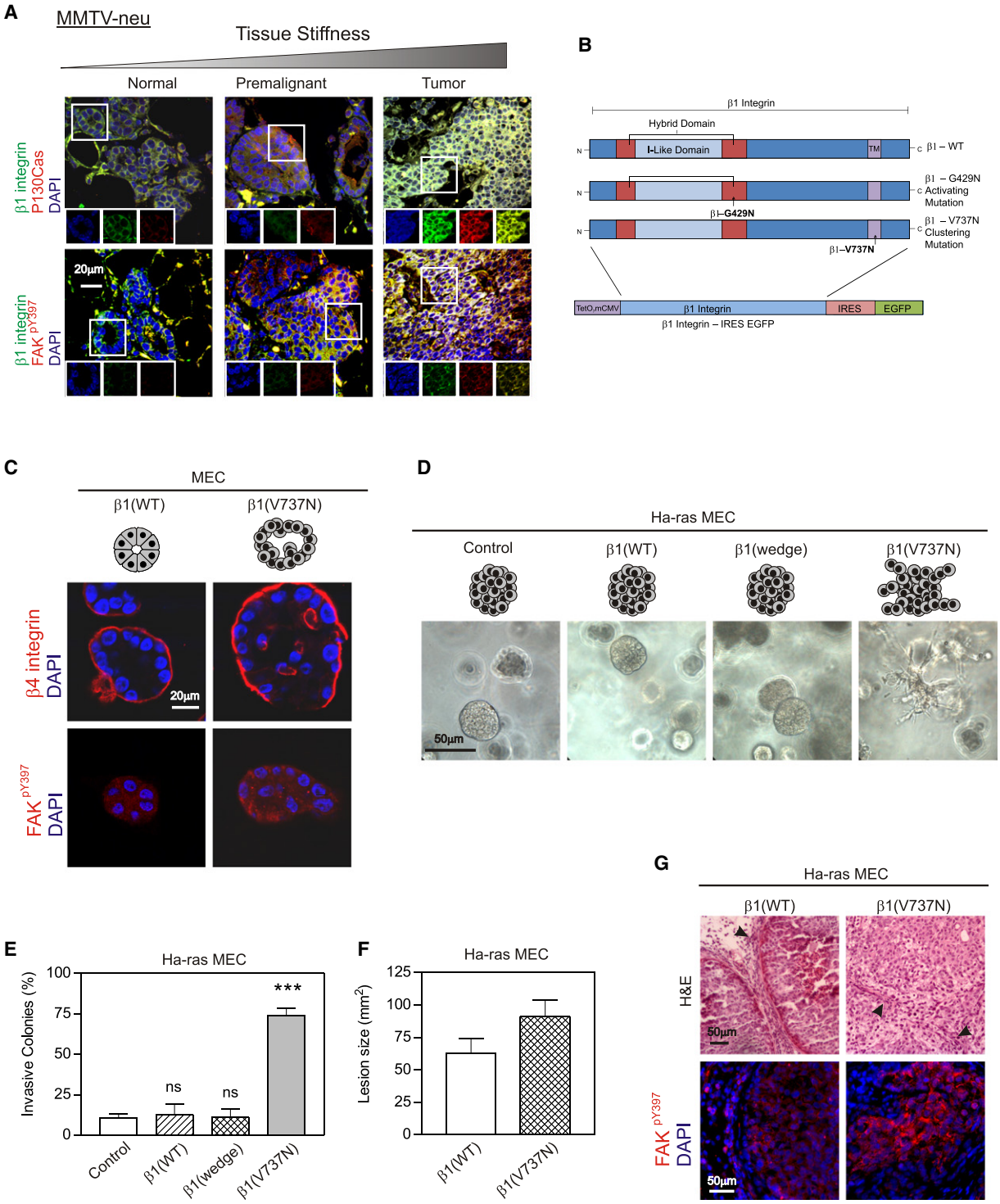

Figure 6. β1 Integrin Clustering Promotes Focal Adhesions and Drives Invasion of a Premalignant Mammary Epithelium in Culture and In Vivo

(A) Combined and split (inserts) confocal images of tissue sections from MMTV-Neu breast stained for DAPI (nuclei, blue) and p130Cas (red, top), or β1 integrin (green, bottom) and activate FAK (FAK^{pY397}, red). The scale bar represents 20 μm. (Colocalization analysis of the malignant tumors: FAK^{pY397} and β1 integrin, Pearson's r = 0.78; ^{p130}Cas and β1 integrin, Pearson's r = 0.89.)

(B) β1 integrin constructs used for the studies shown in (C)–(G).

(C) Confocal images of MCF10A MEC rBM colonies expressing the β1 integrin wild-type [β1(WT)] or clustering mutant [β1(V737N)] stained for β4 integrin (red, top), active FAK (FAK^{pY397}, red, bottom) and DAPI (nuclei, blue).

fat pads. All mice were sacrificed at 8 weeks of age (3 weeks after MEC injection and 5 weeks after fibroblast injection), lesion volume was assessed by caliper measurement, photographed in situ, and dissected gland fragments were imaged and mechanically tested or snap frozen, or fixed and paraffin embedded.

Subcutaneous Studies

Proliferating rBM-generated organoids (16–20 cells/organoid) from each experimental condition were injected subcutaneously into the rear flanks of BalbC nu/nu mice (six to eight mice/group; 5–10 × 10^6), tumor formation was monitored for 3 weeks, and samples were assessed as above at study termination.

Collagen Crosslinking

Mammary gland collagen was reduced with standardized NaB^3H_4, hydrolyzed with 6N HCl, and subjected to amino acid and collagen crosslink analyses as described (Yamauchi and Shiiba, 2008) (Supplemental Experimental Procedures). The reducible crosslinks, dehydro-dihydroxylysinonorleucine (deH-DHLNL) and deH-hydroxylysinonorleucine (deH-HLNL), their ketoamines, were identified as their reduced forms, i.e., DHLNL and HLNL. The crosslinks analyzed (reducible and nonreducible) were quantified as moles/mole of collagen based on the hydroxyproline value of 300 residues per collagen molecule. LOX activity was measured in cell supernatant and plasma as described (Erler et al., 2006).

Immunostaining and Imaging

Immunofluorescence and imaging of 3D cultures and tissues was as described (Paszek et al., 2005). Picrosirius red analysis was achieved through the use of paraffin sections of mammary glands stained with 0.1% picrosirius red (Direct Red 80, Sigma) and counterstained with Weigert's hematoxylin to reveal fibrillar collagen. Sections were serially imaged with an Olympus IX81 fluorescence microscope fitted with an analyzer (U-ANT) and polarizer (U-POT, Olympus) oriented parallel and orthogonal to each other and quantified with minimal thresholding. Two-photon second harmonics imaging was performed on a Prairie Technology Ultima System attached to an Olympus BX-51 with a water immersion objective, and samples were quantified by calculation of the linearity of multiple collagen fibrils (see the Supplemental Data for further details).

Immunoblot Analysis

Cells were lysed in RIPA or Laemmli buffer and assayed by immunoblotting (Johnson et al., 2007).

Statistics

Statistical analysis was performed with GraphPad Prism with an unpaired student's t test, two-way ANOVA, or Fisher's exact test.

SUPPLEMENTAL DATA

Supplemental Data include Supplemental Experimental Procedures and 11 figures and can be found with this article online at http://www.cell.com/supplemental/S0092-8674(09)01353-1.

ACKNOWLEDGMENTS

We thank K. Ignatoski for the ErbB2 construct, M.P. Marinkovich for the BM165 antibody, P. Mrass for two-photon microscopy guidance, and R.G. Wells for mentoring of K.R.L. The work was supported by grants NIH R01-CA078731, DOD W81XWH-05-1-330, DOE A107165, CIRM RS1-00449, and NCI U54CA143836 to V.M.W. NIH T32HL00795404 supported K.R.L., and NIH R01-CA057621 supported M.E.

Received: January 8, 2009
Revised: July 14, 2009
Accepted: September 28, 2009
Published online: November 19, 2009

REFERENCES

Atsawasuwan, P., Mochida, Y., Katafuchi, M., Kaku, M., Fong, K.S., Csiszar, K., and Yamauchi, M. (2008). Lysyl oxidase binds transforming growth factor-beta and regulates its signaling via amine oxidase activity. J. Biol. Chem. *283*, 34229–34240.

Bierie, B., and Moses, H.L. (2006). Tumour microenvironment: TGFbeta: the molecular Jekyll and Hyde of cancer. Nat. Rev. Cancer *6*, 506–520.

Bierie, B., Chung, C.H., Parker, J.S., Stover, D.G., Cheng, N., Chytil, A., Aakre, M., Shyr, Y., and Moses, H.L. (2009). Abrogation of TGF-beta signaling enhances chemokine production and correlates with prognosis in human breast cancer. J. Clin. Invest. *119*, 1571–1582.

Bondareva, A., Downey, C.M., Ayres, F., Liu, W., Boyd, S.K., Hallgrimsson, B., and Jirik, F.R. (2009). The lysyl oxidase inhibitor, beta-aminopropionitrile, diminishes the metastatic colonization potential of circulating breast cancer cells. PLoS ONE *4*, e5620.

Butcher, D.T., Alliston, T., and Weaver, V.M. (2009). A tense situation: forcing tumour progression. Nat. Rev. Cancer *9*, 108–122.

Cabodi, S., Tinnirello, A., Di Stefano, P., Bisaro, B., Ambrosino, E., Castellano, I., Sapino, A., Arisio, R., Cavallo, F., Forni, G., et al. (2006). p130Cas as a new regulator of mammary epithelial cell proliferation, survival, and HER2-neu oncogene-dependent breast tumorigenesis. Cancer Res. *66*, 4672–4680.

Colpaert, C.G., Vermeulen, P.B., Fox, S.B., Harris, A.L., Dirix, L.Y., and Van Marck, E.A. (2003). The presence of a fibrotic focus in invasive breast carcinoma correlates with the expression of carbonic anhydrase IX and is a marker of hypoxia and poor prognosis. Breast Cancer Res. Treat. *81*, 137–147.

Coussens, L.M., Raymond, W.W., Bergers, G., Laig-Webster, M., Behrendtsen, O., Werb, Z., Caughey, G.H., and Hanahan, D. (1999). Inflammatory mast cells up-regulate angiogenesis during squamous epithelial carcinogenesis. Genes Dev. *13*, 1382–1397.

Coussens, L.M., Fingleton, B., and Matrisian, L.M. (2002). Matrix metalloproteinase inhibitors and cancer: trials and tribulations. Science *295*, 2387–2392.

Csiszar, K. (2001). Lysyl oxidases: a novel multifunctional amine oxidase family. Prog. Nucleic Acid Res. Mol. Biol. *70*, 1–32.

Decitre, M., Gleyzal, C., Raccurt, M., Peyrol, S., Aubert-Foucher, E., Csiszar, K., and Sommer, P. (1998). Lysyl oxidase-like protein localizes to sites of de novo fibrinogenesis in fibrosis and in the early stromal reaction of ductal breast carcinomas. Lab. Invest. *78*, 143–151.

Erler, J.T., and Giaccia, A.J. (2006). Lysyl oxidase mediates hypoxic control of metastasis. Cancer Res. *66*, 10238–10241.

Erler, J.T., and Weaver, V.M. (2009). Three-dimensional context regulation of metastasis. Clin. Exp. Metastasis *26*, 35–49.

Erler, J.T., Bennewith, K.L., Nicolau, M., Dornhofer, N., Kong, C., Le, Q.T., Chi, J.T., Jeffrey, S.S., and Giaccia, A.J. (2006). Lysyl oxidase is essential for hypoxia-induced metastasis. Nature *440*, 1222–1226.

(D) Phase-contrast images of Ha-ras MCF10AT MEC colonies expressing the β1 integrin wild-type, glycan wedge, or integrin cluster mutant in rBM. The scale bar represents 50 μm.
(E) Percent invasion of the colonies shown in (D).
(F) Lesion size formed by Ha-ras MCF10AT MECs expressing the clustering β1 integrin mutation [β1(V737N)] and wild-type integrin [β1(WT)].
(G) Top panels: photomicrographs of H&E-stained sections of tumors formed by Ha-ras MECs expressing the clustering β1 integrin mutation [β1(V737N)] and wild-type integrin [β1(WT)]. Bottom panels: confocal images of tissues stained for active FAK (FAK^{pY397}, red) and DAPI (nuclei, blue). Scale bars represent 50 μm. Values in (E) and (F) are shown as mean ± SEM from 12–50 measurements/three experiments. ***$p \leq 0.001$.

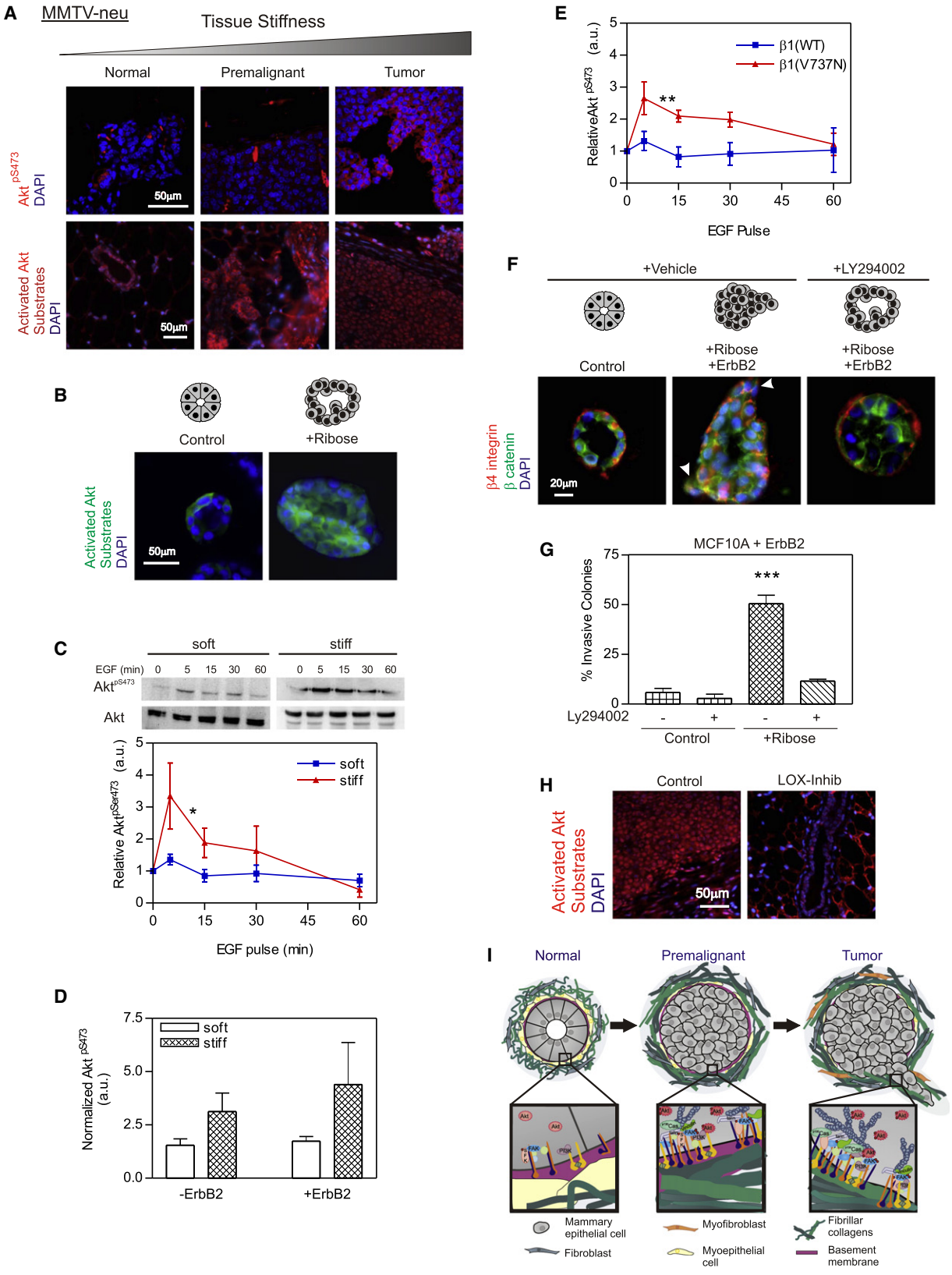
A
MMTV-neu
Tissue Stiffness
Normal
Premalignant
Tumor
Akt pS473 DAPI
Activated Akt Substrates DAPI
50μm
B
Control
+Ribose
Activated Akt Substrates DAPI
50μm
C
soft
stiff
EGF (min) 0 5 15 30 60 0 5 15 30 60
Akt pS473
Akt
Relative Akt pSer473 (a.u.)
EGF pulse (min)
D
soft
stiff
Normalized Akt pS473 (a.u.)
-ErbB2
+ErbB2
E
β1(WT)
β1(V737N)
RelativeAkt pS473 (a.u.)
EGF Pulse
F
+Vehicle
+LY294002
Control
+Ribose +ErbB2
+Ribose +ErbB2
β4 integrin
β catenin
DAPI
20μm
G
MCF10A + ErbB2
% Invasive Colonies
Ly294002
Control
+Ribose
H
Control
LOX-Inhib
Activated Akt Substrates DAPI
50μm
I
Normal
Premalignant
Tumor
Mammary epithelial cell
Fibroblast
Myofibroblast
Myoepithelial cell
Fibrillar collagens
Basement membrane

Erler, J.T., Bennewith, K.L., Cox, T.R., Lang, G., Bird, D., Koong, A., Le, Q.T., and Giaccia, A.J. (2009). Hypoxia-induced lysyl oxidase is a critical mediator of bone marrow cell recruitment to form the premetastatic niche. Cancer Cell *15*, 35–44.

Georges, P.C., Hui, J.J., Gombos, Z., McCormick, M.E., Wang, A.Y., Uemura, M., Mick, R., Janmey, P.A., Furth, E.E., and Wells, R.G. (2007). Increased stiffness of the rat liver precedes matrix deposition: implications for fibrosis. Am. J. Physiol. Gastrointest. Liver Physiol. *293*, G1147–G1154.

Girton, T.S., Oegema, T.R., and Tranquillo, R.T. (1999). Exploiting glycation to stiffen and strengthen tissue equivalents for tissue engineering. J. Biomed. Mater. Res. *46*, 87–92.

Hasebe, T., Tsuda, H., Tsubono, Y., Imoto, S., and Mukai, K. (1997). Fibrotic focus in invasive ductal carcinoma of the breast: a histopathological prognostic parameter for tumor recurrence and tumor death within three years after the initial operation. Jpn. J. Cancer Res. *88*, 590–599.

Hu, M., Yao, J., Carroll, D.K., Weremowicz, S., Chen, H., Carrasco, D., Richardson, A., Violette, S., Nikolskaya, T., Nikolsky, Y., et al. (2008). Regulation of in situ to invasive breast carcinoma transition. Cancer Cell *13*, 394–406.

Jodele, S., Blavier, L., Yoon, J.M., and DeClerck, Y.A. (2006). Modifying the soil to affect the seed: role of stromal-derived matrix metalloproteinases in cancer progression. Cancer Metastasis Rev. *25*, 35–43.

Johnson, K.R., Leight, J.L., and Weaver, V.M. (2007). Demystifying the effects of a three-dimensional microenvironment in tissue morphogenesis. Methods Cell Biol. *83*, 547–583.

Kagan, H.M., and Li, W. (2003). Lysyl oxidase: properties, specificity, and biological roles inside and outside of the cell. J. Cell. Biochem. *88*, 660–672.

Katz, M., Amit, I., Citri, A., Shay, T., Carvalho, S., Lavi, S., Milanezi, F., Lyass, L., Amariglio, N., Jacob-Hirsch, J., et al. (2007). A reciprocal tensin-3-cten switch mediates EGF-driven mammary cell migration. Nat. Cell Biol. *9*, 961–969.

Kim, H., and Muller, W.J. (1999). The role of the epidermal growth factor receptor family in mammary tumorigenesis and metastasis. Exp. Cell Res. *253*, 78–87.

Kirschmann, D.A., Seftor, E.A., Fong, S.F., Nieva, D.R., Sullivan, C.M., Edwards, E.M., Sommer, P., Csiszar, K., and Hendrix, M.J. (2002). A molecular role for lysyl oxidase in breast cancer invasion. Cancer Res. *62*, 4478–4483.

Kolacna, L., Bakesova, J., Varga, F., Kostakova, E., Planka, L., Necas, A., Lukas, D., Amler, E., and Pelouch, V. (2007). Biochemical and biophysical aspects of collagen nanostructure in the extracellular matrix. Physiol. Res. *56* (*Suppl 1*), S51–S60.

Koukoulis, G.K., Howeedy, A.A., Korhonen, M., Virtanen, I., and Gould, V.E. (1993). Distribution of tenascin, cellular fibronectins and integrins in the normal, hyperplastic and neoplastic breast. J. Submicrosc. Cytol. Pathol. *25*, 285–295.

Kuperwasser, C., Chavarria, T., Wu, M., Magrane, G., Gray, J.W., Carey, L., Richardson, A., and Weinberg, R.A. (2004). Reconstruction of functionally normal and malignant human breast tissues in mice. Proc. Natl. Acad. Sci. USA *101*, 4966–4971.

Lahlou, H., Sanguin-Gendreau, V., Zuo, D., Cardiff, R.D., McLean, G.W., Frame, M.C., and Muller, W.J. (2007). Mammary epithelial-specific disruption of the focal adhesion kinase blocks mammary tumor progression. Proc. Natl. Acad. Sci. USA *104*, 20302–20307.

Lo, C.M., Wang, H.B., Dembo, M., and Wang, Y.L. (2000). Cell movement is guided by the rigidity of the substrate. Biophys. J. *79*, 144–152.

Lucero, H.A., and Kagan, H.M. (2006). Lysyl oxidase: an oxidative enzyme and effector of cell function. Cell. Mol. Life Sci. *63*, 2304–2316.

Madan, R., Smolkin, M.B., Cocker, R., Fayyad, R., and Oktay, M.H. (2006). Focal adhesion proteins as markers of malignant transformation and prognostic indicators in breast carcinoma. Hum. Pathol. *37*, 9–15.

Martin, L.J., and Boyd, N.F. (2008). Mammographic density. Potential mechanisms of breast cancer risk associated with mammographic density: hypotheses based on epidemiological evidence. Breast Cancer Res. *10*, 201.

Martin, M.D., Carter, K.J., Jean-Philippe, S.R., Chang, M., Mobashery, S., Thiolloy, S., Lynch, C.C., Matrisian, L.M., and Fingleton, B. (2008). Effect of ablation or inhibition of stromal matrix metalloproteinase-9 on lung metastasis in a breast cancer model is dependent on genetic background. Cancer Res. *68*, 6251–6259.

Miranti, C.K., and Brugge, J.S. (2002). Sensing the environment: a historical perspective on integrin signal transduction. Nat. Cell Biol. *4*, E83–E90.

Mitra, S.K., and Schlaepfer, D.D. (2006). Integrin-regulated FAK-Src signaling in normal and cancer cells. Curr. Opin. Cell Biol. *18*, 516–523.

Muthuswamy, S.K., Li, D., Lelievre, S., Bissell, M.J., and Brugge, J.S. (2001). ErbB2, but not ErbB1, reinitiates proliferation and induces luminal repopulation in epithelial acini. Nat. Cell Biol. *3*, 785–792.

Oleggini, R., Gastaldo, N., and Di Donato, A. (2007). Regulation of elastin promoter by lysyl oxidase and growth factors: cross control of lysyl oxidase on TGF-beta1 effects. Matrix Biol. *26*, 494–505.

Page-McCaw, A., Ewald, A.J., and Werb, Z. (2007). Matrix metalloproteinases and the regulation of tissue remodelling. Nat. Rev. Mol. Cell Biol. *8*, 221–233.

Paszek, M.J., Zahir, N., Johnson, K.R., Lakins, J.N., Rozenberg, G.I., Gefen, A., Reinhart-King, C.A., Margulies, S.S., Dembo, M., Boettiger, D., et al. (2005). Tensional homeostasis and the malignant phenotype. Cancer Cell *8*, 241–254.

Payne, S.L., Hendrix, M.J., and Kirschmann, D.A. (2007). Paradoxical roles for lysyl oxidases in cancer–a prospect. J. Cell. Biochem. *101*, 1338–1354.

Pfeiffer, B.J., Franklin, C.L., Hsieh, F.H., Bank, R.A., and Phillips, C.L. (2005). Alpha 2(I) collagen deficient oim mice have altered biomechanical integrity, collagen content, and collagen crosslinking of their thoracic aorta. Matrix Biol. *24*, 451–458.

Figure 7. Tissue Stiffness Promotes Integrin Clustering and Enhances Growth Factor-Dependent PI3K Activation

(A) Confocal images of tissue from MMTV-Neu breast stained for activated Akt^{pS473} (red, top panels), active Akt substrate (red, bottom panels) and DAPI (nuclei, blue). Scale bars represent 50 μm.

(B) Confocal images of MEC colonies in untreated (Control) or ribose-crosslinked (+Ribose) collagen/rBM gels stained for active Akt substrate (green) and DAPI (nuclei, blue). The scale bar represents 50 μm.

(C) Immunoblots and line graph of time course of Akt^{pS473} and total Akt in EG-treated MCF10A MECs on soft and stiff rBM-PA gels.

(D) Ratio of Akt^{pS473} to total Akt in MCF10A MECS with active (+ErbB2, Dox induced) and nonactive (−ErbB2, noninduced) wild-type ErbB2 on soft and stiff rBM-PA gels.

(E) Time course of EGF activated Akt^{pS473} to total Akt in MCF10A MECs expressing the wild-type β1 integrin [β1(WT)] or the β1 integrin cluster mutant [β1(V737N)] on soft rBM-PA gels.

(F) Confocal images of MCF10A MEC colonies stained for β catenin (green), β4 integrin (red), and DAPI (nuclei, blue) in control or ribose-crosslinked collagen/rBM gels in the presence (+ErbB2) or absence of doxycycline, with or without the PI3K inhibitor, LY294002. The scale bar represents 20 μm.

(G) Quantification of invasive colonies from (F).

(H) Confocal images of sections from control and LOX-inhibited Neu mice stained for active Akt substrate (red) and DAPI (nuclei, blue). The scale bar represents 50 μm.

(I) Cartoon showing effect of ECM stiffness on mammary colony behavior.

Values in (C), (D), and (E) are shown as mean ± SEM of three experiments, 50–100 colonies/experiment. *$p \leq 0.05$, **$p \leq 0.01$, ***$p \leq 0.001$.

Postovit, L.M., Abbott, D.E., Payne, S.L., Wheaton, W.W., Margaryan, N.V., Sullivan, R., Jansen, M.K., Csiszar, K., Hendrix, M.J., and Kirschmann, D.A. (2008). Hypoxia/reoxygenation: a dynamic regulator of lysyl oxidase-facilitated breast cancer migration. J. Cell. Biochem. *103*, 1369–1378.

Ramaswamy, S., Ross, K.N., Lander, E.S., and Golub, T.R. (2003). A molecular signature of metastasis in primary solid tumors. Nat. Genet. *33*, 49–54.

Sawada, Y., Tamada, M., Dubin-Thaler, B.J., Cherniavskaya, O., Sakai, R., Tanaka, S., and Sheetz, M.P. (2006). Force sensing by mechanical extension of the Src family kinase substrate p130Cas. Cell *127*, 1015–1026.

Sinkus, R., Lorenzen, J., Schrader, D., Lorenzen, M., Dargatz, M., and Holz, D. (2000). High-resolution tensor MR elastography for breast tumour detection. Phys. Med. Biol. *45*, 1649–1664.

Sternlicht, M.D., Lochter, A., Sympson, C.J., Huey, B., Rougier, J.P., Gray, J.W., Pinkel, D., Bissell, M.J., and Werb, Z. (1999). The stromal proteinase MMP3/stromelysin-1 promotes mammary carcinogenesis. Cell *98*, 137–146.

Szauter, K.M., Cao, T., Boyd, C.D., and Csiszar, K. (2005). Lysyl oxidase in development, aging and pathologies of the skin. Pathol. Biol. (Paris) *53*, 448–456.

Tetu, B., Brisson, J., Wang, C.S., Lapointe, H., Beaudry, G., Blanchette, C., and Trudel, D. (2006). The influence of MMP-14, TIMP-2 and MMP-2 expression on breast cancer prognosis. Breast Cancer Res. *8*, R28.

Tschumperlin, D.J., Dai, G., Maly, I.V., Kikuchi, T., Laiho, L.H., McVittie, A.K., Haley, K.J., Lilly, C.M., So, P.T., Lauffenburger, D.A., et al. (2004). Mechanotransduction through growth-factor shedding into the extracellular space. Nature *429*, 83–86.

van der Slot, A.J., van Dura, E.A., de Wit, E.C., De Groot, J., Huizinga, T.W., Bank, R.A., and Zuurmond, A.M. (2005). Elevated formation of pyridinoline cross-links by profibrotic cytokines is associated with enhanced lysyl hydroxylase 2b levels. Biochim. Biophys. Acta *1741*, 95–102.

Webster, M.A., Hutchinson, J.N., Rauh, M.J., Muthuswamy, S.K., Anton, M., Tortorice, C.G., Cardiff, R.D., Graham, F.L., Hassell, J.A., and Muller, W.J. (1998). Requirement for both Shc and phosphatidylinositol 3′ kinase signaling pathways in polyomavirus middle T-mediated mammary tumorigenesis. Mol. Cell. Biol. *18*, 2344–2359.

White, D.E., Kurpios, N.A., Zuo, D., Hassell, J.A., Blaess, S., Mueller, U., and Muller, W.J. (2004). Targeted disruption of beta1-integrin in a transgenic mouse model of human breast cancer reveals an essential role in mammary tumor induction. Cancer Cell *6*, 159–170.

Wipff, P.J., Rifkin, D.B., Meister, J.J., and Hinz, B. (2007). Myofibroblast contraction activates latent TGF-beta1 from the extracellular matrix. J. Cell Biol. *179*, 1311–1323.

Wolf, K., Wu, Y.I., Liu, Y., Geiger, J., Tam, E., Overall, C., Stack, M.S., and Friedl, P. (2007). Multi-step pericellular proteolysis controls the transition from individual to collective cancer cell invasion. Nat. Cell Biol. *9*, 893–904.

Yamauchi, M., and Shiiba, M. (2008). Lysine hydroxylation and cross-linking of collagen. Methods Mol. Biol. *446*, 95–108.

Zaman, M.H., Trapani, L.M., Sieminski, A.L., Mackellar, D., Gong, H., Kamm, R.D., Wells, A., Lauffenburger, D.A., and Matsudaira, P. (2006). Migration of tumor cells in 3D matrices is governed by matrix stiffness along with cell-matrix adhesion and proteolysis. Proc. Natl. Acad. Sci. USA *103*, 10889–10894.

Zhang, B., Cao, X., Liu, Y., Cao, W., Zhang, F., Zhang, S., Li, H., Ning, L., Fu, L., Niu, Y., et al. (2008). Tumor-derived matrix metalloproteinase-13 (MMP-13) correlates with poor prognoses of invasive breast cancer. BMC Cancer *8*, 83.

Zhao, Y., Min, C., Vora, S., Trackman, P.C., Sonenshein, G.E., and Kirsch, K.H. (2008). The lysyl oxidase pro-peptide attenuates fibronectin-mediated activation of focal adhesion kinase and p130Cas in breast cancer cells. J. Biol. Chem. *284*, 1385–1393.

Zutter, M.M., Sun, H., and Santoro, S.A. (1998). Altered integrin expression and the malignant phenotype: the contribution of multiple integrated integrin receptors. J. Mammary Gland Biol. Neoplasia *3*, 191–200.